Colloids and Surfaces A: Physicochemical and Engineering Aspects 671 (2023) 131622

Contents lists available at ScienceDirect

Colloids and Surfaces A: Physicochemical and Engineering Aspects

journal homepage: www.elsevier.com/locate/colsurfa

# Formation and characterisation of concentrated emulsion gels stabilised by faba bean protein isolate and its applications for 3D food printing

Yinxuan Hu [a], Lirong Cheng [b], Sung Je Lee [a], Zhi Yang [a,*]

[a] School of Food and Advanced Technology, Massey University, Auckland 0632, New Zealand
[b] The Riddet Institute, Massey University, Palmerston North 4472, New Zealand

## GRAPHICAL ABSTRACT

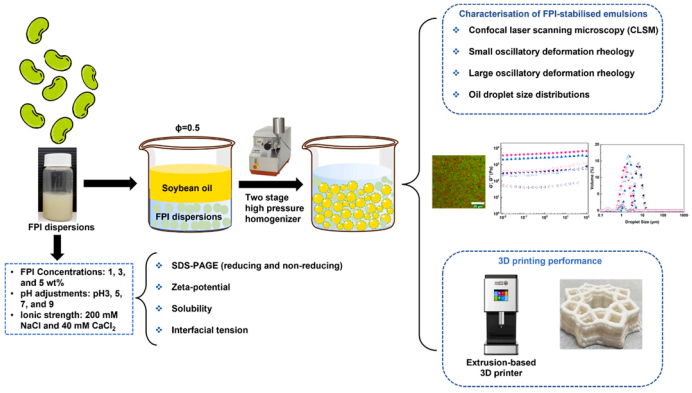


## ARTICLE INFO

*Keywords:*
Emulsion gel
Faba bean protein isolate
3D Printing
Viscoelasticity
Microstructures

## ABSTRACT

Concentrated emulsions were prepared at a fixed oil concentration (50 wt%) using faba bean protein isolates (FPI) as an emulsifier and texturizer. Effects of FPI concentration (1, 3 and 5 wt%; at pH7), pH (pH 3, 5, 7, and 9; 3 wt%) and addition of salts (200 mM NaCl and 40 mM $CaCl_2$; at 3 wt% FPI and pH 7) on the emulsion formation were studied. The oil droplet size and microstructural characteristics were examined by static light scattering and confocal laser scanning microscopy (CLSM), and the viscoelastic behaviours of emulsions were characterised by oscillatory rheology. At all different FPI concentrations, the emulsions formed viscoelastic gels with different gel strengths and stability due to network formation and interactions between jammed oil droplets and protein aggregates. The oil droplet size, rheological properties, and 3D printability of emulsions were not significantly changed by the presence of salts. The storage modulus $G'$ (1 Hz) values were higher at higher FPI concentrations, and higher pH values (i.e., pH 7 and 9) as the droplet size was smaller and the droplet packing was more compact, resulting in a better 3D printing performance. Furthermore, the heat treatment (90 °C for 30 min) remarkedly improved gel strength and the 3D printability because of protein denaturation and oil droplet aggregation. This finding demonstrated that the emulsion gel formed with FPI was tuneable for food 3D printing.

* Corresponding author.
*E-mail address:* Z.Yang2@massey.ac.nz (Z. Yang).

https://doi.org/10.1016/j.colsurfa.2023.131622
Received 20 March 2023; Received in revised form 30 April 2023; Accepted 6 May 2023
Available online 10 May 2023

Most of samples displayed high printing precision with great self-supporting capability, which may find potential applications in creating specialised diet.

## 1. Introduction

Extrusion-based 3D food printing is an additive manufacturing method for fabricating layer-by-layer solid geometries from edible materials via digital models [1]. Aside from creating complex structures, food 3D printing can also be used to formulate customised nutritional food formulations for consumers with different needs and preferences [1]. For example, 3D-printed foods can enhance children's curiosity towards vegetable-based foods by building fancy food shapes, providing more appealing foods for the elderly with swallowing difficulties, and creating controllable delivery systems for medication and nutrients [2]. However, extrusion printing requires food inks to have shear-thinning behaviour and ideal mechanical properties (e.g., $G' > 1000$ Pa) [3,4]. The printable food inks should flow easily through a nozzle tip and develop well-defined geometries [5].

Recently, food emulsion gels have been widely used in food 3D printing to create fat replacements [6], customised diets [7], and encapsulation of functional components [7]. Gels are soft solid-like materials with a three-dimensional network structure [8,9] and emulsion gels are composite structures consisting of oil droplets within a gel matrix [10,11]. Due to the emulsion gel's unique structure and mechanical properties, it has recently attracted considerable attention due to its potential applications as printable 3D food inks [3]. However, most of emulsion gels used for food 3D printing are high internal phase emulsions (HIPEs) with a high oil content (e.g. $\varphi > 0.74$) [12], which is not healthy. In addition, most of them showed weak self-supporting behaviour after 3D printing [13].

Food proteins particularly from animal origins such as gelatine [14] and whey protein isolates (WPI) [15] have been extensively used for fabrication of emulsion gels. Nowadays, a strategy has been taken to reduce animal protein production's ecological footprint by increasing the intake of plant proteins in the human diet [16]. Faba bean (*Vicia faba*) is a promising alternative protein source because of its rich protein content (ranging from 27%−34%) and widely grown around the world [17]. Faba bean protein isolate (FPI) is an underutilised functional protein source with many technofunctional properties, such as water and fat binding, foaming, and gelation capacities [18]. It has been reported that FPI showed better emulsifying properties compared to other plant proteins such as pea protein isolates [19–21] and lentil proteins [22]. Therefore, it is expected that FPI could be suitable for fabrication of vegetarian emulsion gels, which may find potential applications as salad dressings, plant-based mayonnaise, and 3D printing inks for creating customised diets. For example, J. Dille et al. (2022) prepared emulsion gels using mixtures of faba bean protein concentrate (FPC) and λ-carrageenan with incorporations of 20% and 30% oil. The gelation is induced by acidification with glucono-δ-lactone (GDL) [23]. Recently, emulsion gels have also been prepared from whole faba bean flour using lactic acid bacterial fermentation or GDL acidification as gelation methods. However, starch removal is required to improve mechanical strength and water holding capability of emulsion gels [24]. To the best of our knowledge, there is no information on preparation of emulsion gels solely stabilised by FPI and apply them in food 3D printing [25,26]. In addition, FPI also showed excellent gelation capabilities [27]. Thus, the novelty of this work lies in the preparation of 'clean-labelled' plant-based emulsion gels solely using FPI as both emulsifiers and texturizers and explore their potential applications in food 3D printing.

In addition, previous studies showed that protein concentrations [28], pH [29], and presence of salts [30] could significantly affect the formation and characteristics of plant protein stabilised emulsion gels. For example, sufficient proteins are required to stabilise oil-water interfaces, which leads to emulsions with smaller oil droplet size with a high stability. pH values and salt (NaCl and $CaCl_2$) additions have substantial influences on particle sizes, solubilities, and electrostatic interactions of protein particles, which in turn affect the emulsification and gelation capabilities of FPI and the formation of emulsion gels. Therefore, the main objective of this work is to investigate the effects of FPI concentrations (1%, 3%, and 5% w/w), different salt additions (200 mM NaCl and 40 mM $CaCl_2$), and pH levels (pH 3, 5, 7 and 9) on formation, physicochemical properties, microstructural characteristics, and 3D printing performances of FPI stabilised emulsion gels containing 50% oil. Also, the impact of heat treatment (90 °C for 30 min) on characteristics and 3D printing of FPI stabilised emulsion gels was explored as the heat treatment is commonly used in food processing as a pasteurisation method. This study provides a new route to fabricate FPI stabilised concentrated emulsion gels and insight into important factors and conditions to be considered for the formation of stable concentrated emulsion gels with desired mechanical properties for 3D food printing.

## 2. Materials and methods

### 2.1. Materials

The faba bean protein isolate (FPI) was purchased from NZ Protein Inc. (Auckland, New Zealand). According to the manufacturer's specification, the FPI contains ~85% w/w protein, ~5.4% w/w fat, less than ~1% w/w sugar and dietary fibre. Chemicals used in this study, including sodium dodecyl sulphate (SDS), NaCl, $CaCl_2$, petroleum ether, Fast Green, Nile Red, acetic acid, low viscosity mineral oil (M5904), HCl, NaOH, and sodium azide were purchased from Sigma-Aldrich (St. Louis, MO, USA). All chemicals are of analytical grade, and Milli-Q water (Millipore, USA) was used throughout sample preparations. Soybean oil was purchased from a local supermarket (Pakn save, Albany, Auckland, New Zealand). The 4 × Laemmli sample buffer, β-mercaptoethanol, 10 ×Tris/Glycine/SDS running buffer, and Coomassie Brilliant Blue R-250 staining solution were purchased from Bio-Rad (Hercules, CA, USA).

### 2.2. Preparation of FPI dispersions

A stock solution of 10 wt% FPI was prepared by dispersing the FPI powder in Milli-Q water containing 0.04 wt% sodium azide as an antimicrobial agent, followed by magnetically stirring (300 rpm) at ~20 °C for 24 h to ensure complete hydration. The pH was adjusted to 7.0 using 1 M NaOH, followed by stirring (500 rpm) for 6 h. Then, the stock FPI solution was stored at 4 °C until use within a week. Different FPI dispersions with different concentrations of FPI (1, 3 and 5 wt%) were prepared by diluting the FPI stock solution in Milli-Q water. The pH of FPI dispersion (3 wt%) was adjusted to different pHs (pH 3, 5, and 9) by 1 M NaOH or 1 M HCl followed by stirring (500 rpm) for 6 h. The pH values were adjusted every 2 h until stable during stirring. The FPI dispersion (3 wt% at pH 7) was also mixed with salt by adding 200 mM NaCl or 40 mM $CaCl_2$. The mixture was stirred by a magnetic stirrer at 20 °C.

### 2.3. Characterisations of FPI dispersions

#### 2.3.1. SDS-PAGE

SDS-PAGE (sodium dodecyl sulphate-polyacrylamide gel electrophoresis) was used to characterise the protein profiles based on their molecular weight under reducing and non-reducing conditions [31–33]. For SDS-PAGE under reducing conditions, 0.15 wt% FPI solution (25 μL) was mixed with 1.25 μL of reducing agent (β-mercaptoethanol) at room temperature (~20 °C). Then, the sample was boiled for 10 min followed

by cooling prior to loading into the Mini-protein TGX precast gel (Bio-Rad, USA) with 15% resolving gel and 4% stacking gel. A PowerPac Basic (Bio-Rad, USA) was used to perform the electrophoresis at a constant voltage of 130 V in a running buffer (10 × Tris/Glycine/SDS running buffer) (Bio-Rad, USA). After electrophoresis, the gels were stained with Coomassie Brilliant Blue R-250 staining solution (Bio-Rad, USA) for 3 h followed by detaining with 10% isopropanol/glacial acetic acid solution overnight via a shaker (OM6, RATEK, Australia). For protein band identification, a mixture of protein standards with different molecular weights (Precision Plus Protein Dual Xtra Standards) (Catalog # 161–0377, Bio-Rad, USA) with a MW range of 10–250 kDa was also used. For non-reducing SDS-PAGE, β-mercaptoethanol was replaced by Milli-Q while the other procedures remained the same.

#### 2.3.2. ζ-potential of FPI dispersions

The zeta (ζ)-potential of FPI solution with different pHs and salt additions was determined at a protein concentration of 0.1% w/w using dynamic laser scattering (DLS) by a Malvern Zetasizer Nano ZS (Malvern Instruments Ltd, Worcestershire, UK). A refractive index of 1.45 and absorption of 0.001 were applied, respectively [34]. The analysis was determined in triplicate.

#### 2.3.3. Oil-water interfacial tension

The interfacial tension of oil droplets in FPI (0.1 wt%) dispersions was determined by a Theta Flex Plus optical tensiometer (Biolin Scientific Instruments, Sweden) using the pendant drop method [28]. The 0.1 wt% FPI dispersions were prepared by diluting 3 wt% FPI dispersion at different pHs and salt concentrations with MQ water with different pHs and salt solutions. An FPI solution (25 μL) was generated at the stainless-steel syringe tip and immersed in soy oil. The change of interfacial tension with time was monitored up to 5000 s and calculated automatically by One Attention software (Biolin Scientific Instruments, Sweden).

#### 2.3.4. Protein solubility

The solubility of FPI in MQ water with different pHs and salt concentrations was determined according to Luo, Cheng, Zhang and Yang [35] with slight modifications. Specifically, the FPI dispersions were centrifuged at 2500 × *g* for 15 min at room temperature (~20 °C) by a benchtop centrifuge (Thermofisher 3000, MO, USA). Then, the soluble protein content in the supernatant was determined using a Bradford Protein Assay Kit (Bio-Rad, USA) using gamma-globulin as the standard and expressed as the concentration of soluble protein in FPI dispersions. A UV-Vis spectrophotometer (Shimadzu 2000, Kyoto, Japan) was used to determine the absorbance of protein solutions at 595 nm. The solubility (%) was calculated using the following equation:

$$\text{Solubility } (\%) = \frac{\text{Protein content in the supernatant } (\text{mg/mL})}{\text{Total protein content before centrifuge } (\text{mg/mL})} \times 100\% \quad (1)$$

### 2.4. Preparation of emulsions

For the preparation of emulsions, all FPI dispersions were mixed with 50% (v/v) soybean oil and then homogenised by a high shear mixer (T10 basic ULTRA-TURRAX®, IKA Corp., Staufen, Germany) with a 10 mm probe (S10N-10 G, IKA, Germany) at 14,000 rpm for 1 min to obtain coarse emulsions. The coarse emulsions were then further homogenised two times via a two-stage high-pressure homogeniser (HPH) (APV 2000, SPX Flow Technology GmbH, Germany) at the pressure of 12 MPa (1st stage)/2 MPa (2nd stage) for the first pass, and 30 MPa (1st stage)/5 MPa (2nd stage) for the second pass. The stock salt solution was added after the first pass of HPH to ensure the uniform dissolution of salts. Then, the emulsions were stored at room temperature (~20 °C) for further tests, which were completed within three days.

### 2.5. Characterisation of emulsions

#### 2.5.1. Oil droplet size

The mean particle size and particle size distribution (PSD) of emulsion oil droplets were measured using a static laser light diffraction technique (Mastersizer 2000, Malvern Instruments Ltd, Worcestershire, UK) which measures a size range of 0.01–3000 μm in diameter. The refractive indices used for soybean oil and the dispersant (water) were 1.47 and 1.33, respectively [36]. The emulsions were mixed with 1% SDS solution at a weight ratio of ~1:15 and incubated overnight at room temperature (~20 °C) before the particle size measurements in order to displace the protein particles from the oil-water interface and break the oil droplet flocs [37]. The mean particle diameter for single oil droplets was represented as the Sauter mean diameter D [2,3].

#### 2.5.2. Flowability of FPI-stabilised emulsions

To visually examine the flowability of FPI-stabilised emulsions, the glass vials containing samples were inverted and left on the bench at room temperature (~20 °C) before the photographs were taken.

#### 2.5.3. Confocal laser scanning microscopy (CLSM)

Confocal laser scanning microscopy (Leica DM 6000B, Germany) was used to observe the microstructure of FPI-stabilised emulsions prepared at various conditions. Fast Green (1% w/v) and Nile Red were used to stain protein and oil phases with a ratio of 500:1 (v/v) and 5000:1 (v/w), respectively. For thermally treated emulsion gels, the emulsions were transferred onto the glass slides sealed with a glass coverslip by nail polish to avoid evaporation. Then, the samples were incubated in an oven (Thermofisher, USA) at 90 °C for 30 min. Fast green and Nile red were excited at laser wavelengths of 633 nm and 561 nm, respectively. All the images were processed with Image J software (NIH, MD, USA).

#### 2.5.4. Small and large oscillatory deformation rheology

Rheological properties of different emulsion gels were characterised by a stress-controlled rheometer (Physica MCR 301, Anton Paar, Austria) using a parallel plate geometry (40 mm in diameter, 1 mm gap). Aliquots of emulsion samples were transferred onto the bottom plate with a wood spatula. The sample was then carefully trimmed before adding low viscosity mineral oil around the edge of the sample to prevent evaporation. The rheological measurements were conducted in the following protocol, and the storage modulus $G'$ and loss modulus $G''$ were recorded during the tests [25]. Firstly, a time sweep measurement was conducted at 1% strain and 1 Hz for 1 h to rebody the emulsion gel network after loading the samples onto the bottom plate of the rheometer. Then, a frequency sweep test was conducted at 1% strain while the frequency was varied from 0.01 to 100 Hz. Finally, the large deformation rheological behaviour of the emulsions was determined by a strain sweep test at a strain amplitude from 0.01% to 1000% and at 1 Hz. For thermally treated samples, a temperature sweep test was conducted by heating the samples from 20 °C to 90 °C at 2 °C/min, maintaining at 90 °C for 30 min, and cooling down to 20 °C at 2 °C/min. The samples were equilibrated at 20 °C for 15 min before conducting small and large deformation rheological tests at 20 °C as mentioned above. All rheological measurements were conducted in duplicate.

### 2.6. 3D printing

3D printing of emulsion gels was performed on a Wiiboox Sweetin chocolate syringe extrusion type printer (Wiiboox, China) using a metal nozzle with a diameter of 0.84 mm. For each sample, emulsion gel (~10 g) was put into the syringe and set into the 3D printer. Printing parameters used were as follows: printing speed 25 mm $s^{-1}$, printing temperature 20 °C, and the layer height of sample 0.5 mm.

### 2.7. Statistical analysis

All the experiments were conducted at least in duplicate, and the results are reported as mean ± standard deviation (SD). All data were analysed using Minitab statistical software (Minitab 19 Statistical Software, USA). The one-way analysis of variance (ANOVA) was applied to analyse the data. The difference between sample mean values was evaluated via a Tukey's test at a significance level of $P < 0.05$.

## 3. Results and discussion

### 3.1. SDS-PAGE of FPI dispersions

The protein profile of FPI was characterised by both non-reducing and reducing SDS-PAGE as shown in Fig. 1. Under non-reducing conditions, an intense and smeared protein band was found in the loading well at the top of the stacking gel, suggesting the presence of large protein complex having a molecular weight larger than 250 kDa [38]. In addition, there were three major protein bands visible at ~73 kDa, ~59 kDa, and ~51 kDa, which could be assigned to convicilin, legumin (11 S), and vicilin (7 S), respectively [34]. Under reducing conditions, the large protein complex band at the top of the gel vanished, together with the appearance of two new intense bands at ~ 37 kDa and ~ 20 kDa. These two bands could be α-legumin and β-legumin, which are cross-linked to form legumin via a disulfide (S-S) bond [27]. In general, FPI protein profiles observed under both non-reducing and reducing conditions were consistent with previous SDS-PAGE studies of faba bean proteins [34,39]. The major protein bands are legumin-type globulins (11 S) and vicilin-type globulins (7 S) (around 70–78% w/w) followed by albumins (2 S) (10–20% w/w) [40,41].

### 3.2. Protein solubility and Zeta potential

Physicochemical properties of proteins such as electrical net charge (ζ-potential), solubility, and interfacial tension are critical in determining the diffusion and adsorption of protein molecules at the oil-water interface as an emulsifier [41,42]. The solubility and ζ-potential of FPI as a function of pH and salt addition are plotted in Fig. 2. It can be estimated that at ~pH 4.5, the net charge was zero (Fig. 2**A**). The isoelectric point of pH 4.5 for FPI agrees with previous studies [34,42]. The lowest solubility among all FPI samples was observed at pH 5 (Fig. 2**B**), which can be explained by its relatively low electrostatic repulsion as indicated by the smallest absolute ζ-potential values. Also, as shown in Fig. 2**B**, the addition of NaCl (200 mM) and $CaCl_2$ (40 mM) decreased the solubility of FPI, which can be attributed to the charge screening effect of salt as evidenced by their low ζ-potential values. The addition of salts could thus reduce the electrostatic repulsion and promote the attraction and aggregation of FPI molecules. Similar behaviours have been reported in previous studies of other plant proteins added with NaCl and $CaCl_2$, including soybean proteins [43], pea proteins [44], and quinoa proteins [32]. In addition, the FPI added with $CaCl_2$ has significantly lower solubility (~6.7%) than the FPI added with NaCl (~12.8%). This could be due to the fact that compared to monovalent salt, the divalent salts are more efficient in inducing protein aggregation by screening charging of protein molecules and promoting the protein cross-linking via salt bridges [32].

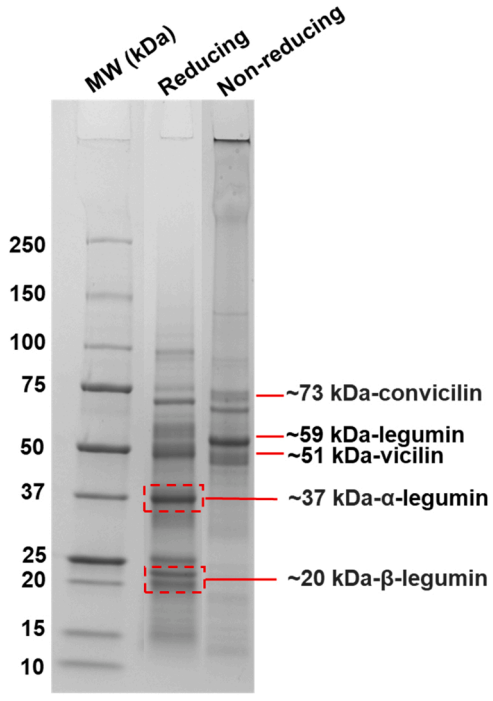


**Fig. 1.** SDS-PAGE profiles of the faba bean protein isolates (FPI) under non-reducing and reducing conditions.

### 3.3. Oil-water interfacial tension

The interfacial tension (IFT) of FPI (3 wt%) at various pHs (3, 5, 7, and 9) as well as FPI with added salts (200 mM NaCl and 40 mM $CaCl_2$) at pH 7 was determined as a function of time by the tensiometer. The interfacial tension of various FPI dispersions as a function of time are shown in Fig. 2**C**. For all FPI samples, the interfacial tension of the protein solutions firstly decreased significantly with time until reaching an equilibrium at ~5000 s. This is a typical characteristic of proteins indicating a stable conformation of protein has been reached after migrating from aqueous phase to adsorb and adopt at the oil-water interface [45]. The equilibrated IFT values at 5000 s of all the samples are shown in Fig. 2**D**. The equilibrated IFT value decreased from ~14.2 mN/m to ~6.9 mN/m when the pH values increased from pH 3 to pH 9, while the final IFT value was the highest (~16.3 mN/m) at pH 5. This indicates that the FPI close to the isoelectric point has the weakest interfacial activity, which could be due to its large aggregate size and minimum solubility. The similar observation has been made in pea protein isolates (PPI) [21].

In addition, it shows that the equilibrated IFT values of FPI were higher at acidic pH than neutral and alkaline pHs. This finding is in line with Keivaninahr, Gadkari, Benis, Tulbek and Ghosh [46], who reported that the IFT value of faba bean protein was higher at pH 2 (~15 mN/m) than pH 7 (~8 mN/m). Similar finding has been found in a IFT study of soybean protein isolate (SPI), where a higher IFT was found at pH 3 (~14 mN/m) compared to pH 7 (~11 mN/m) [47]. In general, it can be observed that protein carrying a higher charge (or with a higher absolute zeta-potential values) is more effective to reduce the interfacial tension and vice versa. A negative correlation between interfacial tension and surface charges have been also observed in previous studies of other plant proteins including SPI, pea protein isolate (PPI), lentil protein isolate (LPI) and canola protein isolate (CPI) at pH 3, 5 and 7 [45].

### 3.4. Microstructural characteristics of emulsion gels

#### 3.4.1. The effect of FPI concentrations

The microstructure and flowability of emulsion gels at various protein concentrations (1, 3, and 5 wt%) before and after heat treatment (90 °C for 30 min) were characterised by using the confocal laser scanning microscopy (CLSM), as shown in Fig. 3.

In CLSM micrographs, the protein phase appears green, while the oil droplets appear red. In all samples, FPI seemed to cover and stabilise the oil droplets. As the FPI concentration increased, the oil droplets of emulsion were smaller with more compact and compressed packing, and the formation of protein aggregates became more obvious. This could lead to stronger gels observed at emulsions stabilised by 3% and 5% FPI

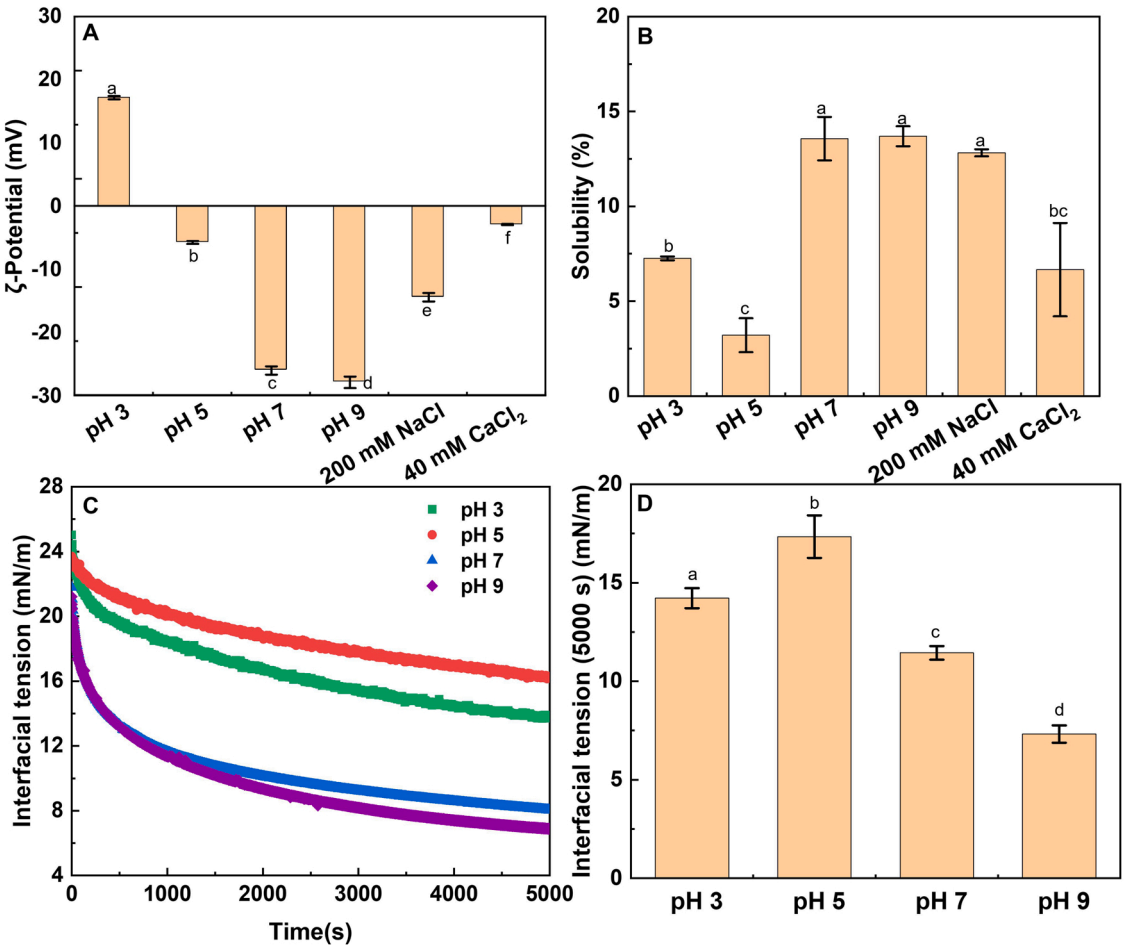


**Fig. 2.** (A) ζ potential of FPI dispersions at different pH values (3−9) and in the presence of 200 mM NaCl and 40 mM $CaCl_2$ at pH 7, (B) solubility of 3 wt% FPI dispersions at different pH values (3−9) and in the presence of 200 mM NaCl or 40 mM $CaCl_2$) at pH 7. (C) Time dependence of oil-water interfacial tension of FPI dispersions at different pH values (3−9) at 20 °C. (D) Final interfacial tension values at 5000 s for all emulsion samples. Different letters above the columns indicate significant difference ($P < 0.05$).

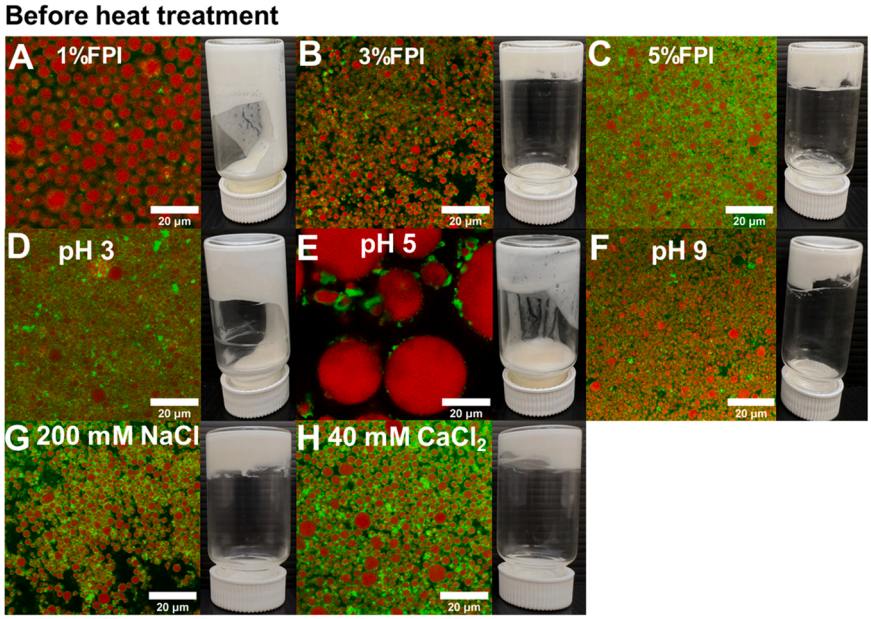


**Fig. 3.** Confocal micrographs and visual appearance of the emulsion samples before heat treatment. (A, B, and C) emulsions stabilised by 1, 3, and 5 wt% of FPI at pH 7. (D, E, and F) emulsions stabilised by 3 wt% of FPI at pH 3, pH 5, and pH 9. (G and F) emulsions stabilised by 3 wt% of FPI at pH 7 in the presence of 200 mM NaCl or 40 mM $CaCl_2$.

as revealed by the tube inversion test [48] **(**Figs. 3**B and** 3**C inset),** where the samples stuck to the bottom of vials and didn't move once inverted. However, 1 wt% FPI stabilised emulsion gel was weak, which flowed to the bottom of the vial after inversion. Similar findings were also reported in previous studies of other plant protein (e.g., quinoa and pea proteins) stabilised emulsions. For example, Zhang et al. (2021) found that the oil droplet size of quinoa protein stabilised emulsion markedly decreased when the quinoa protein concentration increased from 1 to 5 wt% [28]. This could be due to the fact that a higher protein concentration could stabilise a larger interfacial area, leading to smaller oil droplet size and their tighter packing behaviour [48].

### 3.4.2. *The effects of pH*

The confocal micrographs and visual appearance of emulsion gels that were prepared from a fixed FPI dispersion (3 wt%) at different levels of pH 3, 5, 7 and 9 before and after heat treatment are shown in Fig. 3. The emulsion stabilised by FPI at pH 3 and 5 showed a lower self-supporting gel strength and visual gel fluidity. In particular, the large oil droplet and protein aggregates can be observed at pH 5 **(**Fig. 3**E).** This could be attributed to the extensive protein aggregation at the pH close to the isoelectric point (pI~4.5) [49], thus leading to inferior emulsification capability as revealed by a high IFT value (Fig. 2**D**). At pH 7 and 9, semi-solid self-supporting emulsion gels were formed as the emulsions remained at the bottom of the vials when inverted (Figs. 3**B and** 3**F insets**). This could be due to the formation of a strong three-dimensional network structure of oil droplets (Figs. 3**B and** 3**F**), preventing the movement of the oil droplets and providing elastic-like properties [49]. This could be due to higher solubilities, large surface charges, lower IFT values, and better emulsification capabilities of FPI particles/molecules at the pHs away from the pI (pH 7 and pH 9).

### 3.4.3. *The effects of salts*

The visual appearance and CLSM micrographs of 3 wt% FPI stabilised emulsions with and without adding salts (NaCl and $CaCl_2$) are shown in Fig. 3 **G-H**. All emulsion samples formed strong self-supporting emulsion gels, regardless the addition of salts. After adding salts, particularly 40 mM $CaCl_2$, prominent protein aggregation and large oil droplet size can be observed. This could be due to charge screening effect of salts which promoted protein attraction and diminished repulsion. Similar observations have been made in other plant proteins such as quinoa protein isolates in the presence of NaCl (20–200 mM) and $CaCl_2$ (20–50 mM) [32].

### 3.4.4. *The effects of heat treatment*

Heat treatments have been extensively used in food processing to ensure food safety, therefore, the heat stability of FPI emulsions is important for their food applications. As shown in the CLSM images and via visual observations (Fig. 4), the oil droplet size and flowability of samples were not significantly changed before and after heat treatment, except for pH 5 (Fig. 4**E**), indicating the structural stability of emulsions against coalescence and creaming [28]. After heating, the interfacial layer became thicker in all heated FPI emulsion gels and the appearance of large protein aggregates between the oil droplets was observed particularly at pH 5 and in the presence of $CaCl_2$. This could be due to the unfolding, denaturation, and aggregation of FPI at a temperature beyond its denaturation temperature (~77–85 °C) [50,51]. This heat induced FPI aggregates may either adsorb at the O/W interface to make the interfacial layer thicker or be present in the aqueous phase as active fillers in between the oil droplets. This could result in a more compacted arrangement of oil droplets, thus providing a solid self-supporting structure of the emulsion gels [3,52]. The alteration in microstructures may lead to changes in rheological properties of FPI emulsion gels, which will be discussed in Section 3.8.

## 3.5. *Oil droplet sizes and distribution of emulsion gels*

The effects of FPI concentration on the oil droplet size distributions is shown in Fig. 5**A and D**. The emulsion stabilised by 1 wt% FPI displayed a bimodal distribution with a major peak at ~8 μm and a minor peak at ~1 μm. With increasing FPI concentration to 5 wt%, the peaks shifted toward smaller sizes to ~ 1 μm and ~ 0.2 μm. The surface mean diameter D [2,3] was plotted as a function of FPI concentration as shown in Fig. 5**D**, indicating the oil droplet size reduction induced by the increase in FPI concentration. It can be observed that the D [2,3] decreased from ~3.8 μm to ~1.6 μm when the FPI concentration was increased from 1 wt% to 5 wt%. This finding was consistent with the CLSM observation **(**Fig. 3**A-C)** as discussed above. Previous studies suggested that an increase in protein concentration could enhance the

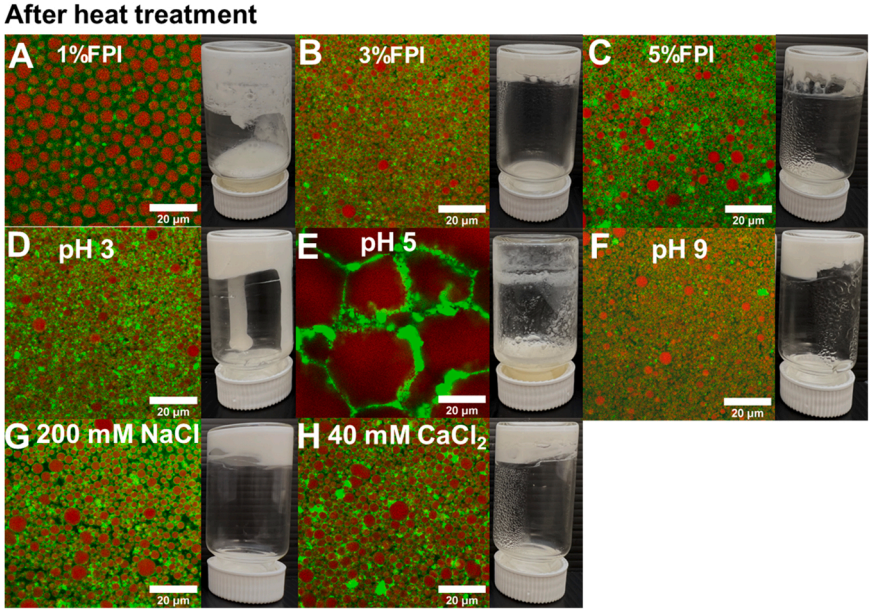


**Fig. 4.** Confocal micrographs and visual appearance of the emulsion samples after heat treatment. (A, B, and C) emulsions stabilised by 1, 3, and 5 wt% of FPI at pH 7. (D, E, and F) emulsions stabilised by 3 wt% of FPI at pH 3, pH 5, and pH 9. (G and F) emulsions stabilised by 3 wt% of FPI at pH 7 in the presence of 200 mM NaCl or 40 mM $CaCl_2$.

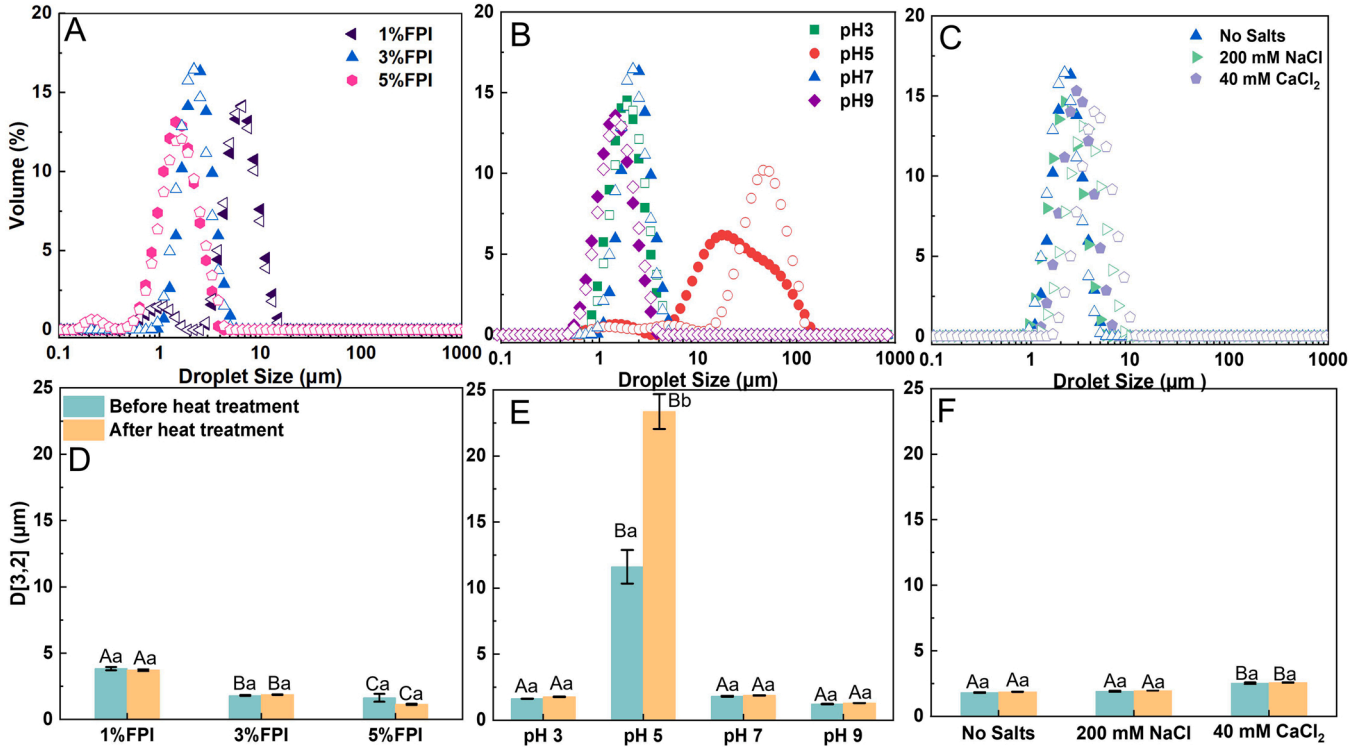


**Fig. 5.** (A, B, and C) Oil droplet size distribution of FPI stabilised emulsion gel before (open symbols) and after heat treatment (solid symbols). (D, E, and F) Sauter mean diameter of oil droplets for all FPI stabilised emulsions. Different capital letters above the columns denote significant differences ($P < 0.05$) in emulsions stabilised by FPI at different concentrations, different pHs or adding with salts. The different lowercase letters denote significant differences ($P < 0.05$) in emulsions before and after heat treatment.

adsorption and surface coverage ability of FPI on oil droplets, thus contributing to stabilising larger interfacial surface areas with limited extent of coalescence [53]. Similar findings have been reported in previous studies on other plant proteins stabilised O/W emulsions. For examples, Xiao, Gonzalez and Huang [54] utilised karifin particles from sorghum to prepare O/W emulsion and indicated that the oil droplet size considerably decreased from ~125 μm to ~40 μm when the concentration of kafirin particles increased from 0.25 wt% to 2 wt%.

The effects of pH of FPI on the oil droplet size distributions and D [2,3] of emulsions are shown in Fig. 5**B and E** , respectively. In general, the oil droplets stabilised by FPI at pH 5 were remarkedly larger (~12 μm) than those at pH 3, 7 and 9, which had comparable oil droplet sizes (~2–2.5 μm). This can be attributed to extensive protein-protein aggregation caused by the reduced electrostatic repulsions near the isoelectric point (pI~4.5) of FPI, so the FPI adsorption layer was ineffective to prevent the aggregation of droplets and the emulsion stability was remarkably decreased [19,49]. The minimum effectiveness of FPI as emulsifiers close to the pI was confirmed with the IFT result, and similar behaviour has been reported in previous studies on O/W emulsions stabilised by pea proteins [55], tomato seed protein isolates [56], and soybean proteins [57]. It has been suggested that proteins with higher stabilities and large surface charges could migrate to the oil-water interface faster to lower interfacial tension and provide charge repulsions once absorbed onto the interface, thereby resulting in smaller oil droplet sizes [49,57].

Salts are usually added to the food emulsions to tune their structural and mechanical properties as well as for micronutrient fortification (e.g. $CaCl_2$). The influence of salt addition (NaCl and $CaCl_2$) on the oil droplet size of FPI stabilised emulsion gels was measured at pH 7 and 3 wt% FPI (Fig. 5**C**). The results showed that the NaCl addition (200 mM) did not induce significant changes in oil droplet size. However, the addition of 40 mM $CaCl_2$ led to a slight increase in oil droplets (from ~1.8 μm to ~2.5 μm). Similar findings were reported in previous studies of SPI stabilised emulsion gels in the presence of 40 mM $CaCl_2$ [58]. In general, the results indicated that divalent salts, such as $CaCl_2$, had larger impact on FPI-stabilised emulsion than monovalent salts such as NaCl, which is in agreement with a previous study of tomato seed protein isolate-stabilised emulsions containing NaCl and $CaCl_2$ [56]. Although the effect of salts on oil droplet size of emulsions depends on the salt type, pH and concentration, it is generally believed that divalent salts have a stronger effect than the monovalent salts [47,54]. This could be due to the strong charge screening and salt bridging effect of $CaCl_2$ than that of NaCl, leading to ion-induced droplet aggregation [32,56].

In line with confocal imaging, the heat treatment did not induce significant changes in the oil droplet size of FPI stabilized emulsions, except at pH 5, indicating a good heat stability. However, the oil droplet size D [2,3] at pH 5 nearly doubled from ~ 12 μm to ~ 24 μm after the heat treatment at 90 °C for 30 min, which was in agreement with the CLSM observations (Fig. 3**E and** Fig. 4**E**). As the oil droplet size was determined after gently mixing with 1 wt% SDS to dissociate the flocculated droplets, the increase in D [2,3] of FPI stabilised emulsion at pH 5 suggests this was possibly due to droplet coalescence rather than aggregation and flocculation [57]. It has been suggested that electrostatic repulsive forces between protein films/particles adsorbed onto the oil droplets are important in stabilizing emulsions against coalescence and flocculation [59]. Therefore, it can be concluded that the emulsion had the lowest thermal stability at pH 5 where the repulsions were minimum.

### *3.6. Small deformation rheological properties of FPI stabilised emulsion gels*

Rheological properties of emulsions are strongly related to their stabilities [60] and 3D printability [61]. The viscoelastic response of all FPI stabilised emulsion gels as a function of frequency is shown in Fig. 6. For all samples, $G'$ and $G''$ were parallel to each other and only slightly

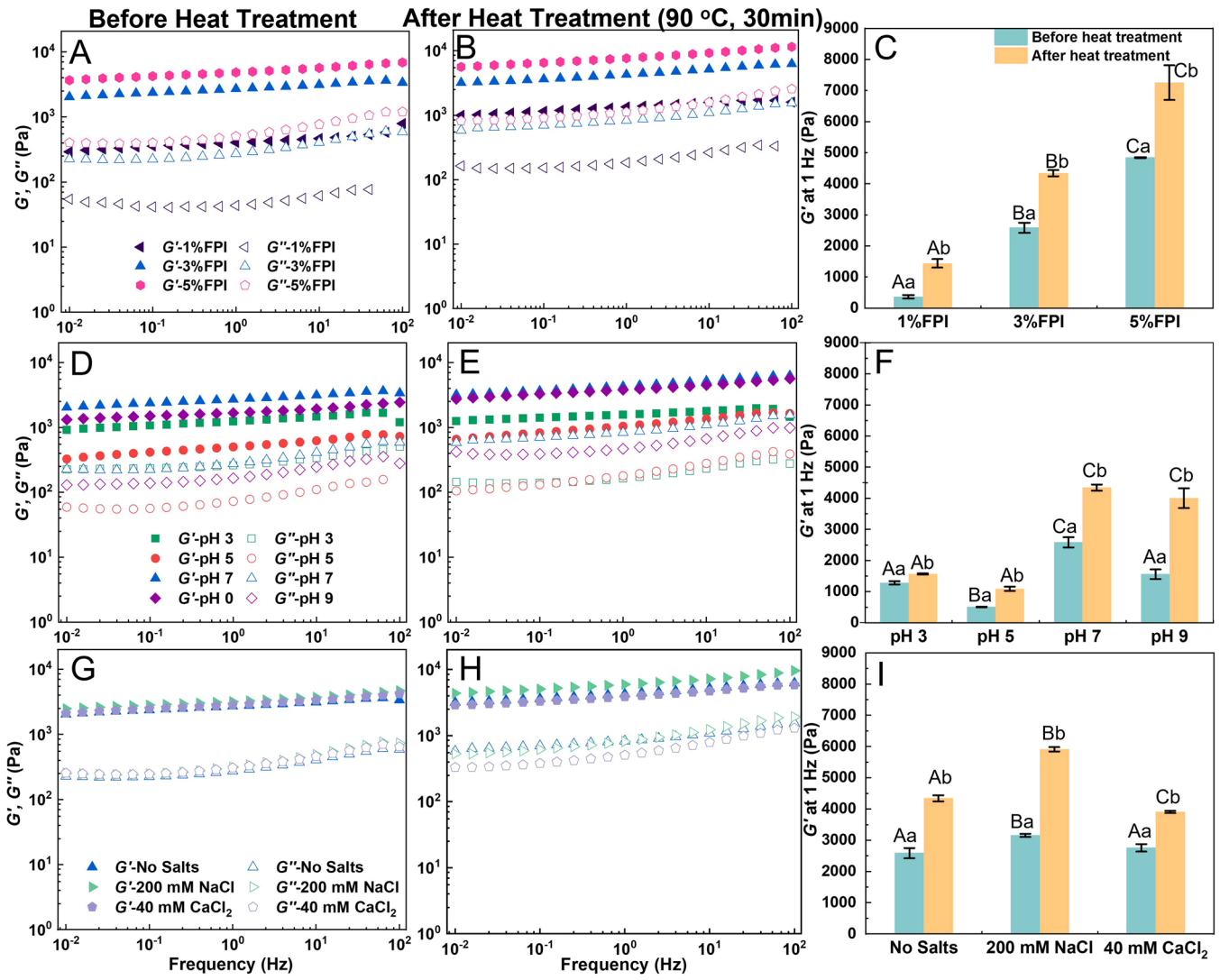


**Fig. 6.** (A and B) The $G'$ (solid symbols) and $G''$ (empty symbols) as a function of frequency for FPI stablisted emulsion gel systems before (A, D, and G) and after (B, E, and H) heat treatment. (C, F, and I) $G'$ (1 Hz) for FPI stabilised emulsions before and after the heat treatment. Different capital letters above the columns denote significant differences ($P < 0.05$) in emulsions stabilised by FPI at different concentrations, different pHs or adding with salts. The different lowercase letters denote significant differences ($P < 0.05$) in emulsions before and after the heat treatment.

changed with frequency. In addition, $G'$ values were almost 10 times higher than $G''$. This suggests that all samples presented a prevailing elastic behaviour that can be considered as gels [62]. The predominantly elastic gel behaviour has been attributed to extensive flocculation process due to interactions among the emulsifiers (i.e., FPI particles/molecules) located at the oil-water interface of adjacent droplets and dense packing of oil droplets [63,64]. Similar findings have been observed in concentrated emulsions stabilised by other plant proteins, such as canola protein-stabilised emulsions (oil fraction $\varphi = 0.5$) [48], and dairy proteins, such as whey protein isolate (WPI)-stabilised emulsions ($\varphi = 0.3$–$0.6$) [65].

To compare the gel strength among all the samples, the $G'$ at 1 Hz is plotted in Fig. 6**C, F, and I.** It is evident that increasing the concentration of FPI led to a greater gel strength of emulsion gels. To be specific, $G'$ (1 Hz) increased from ~365 Pa to ~4840 Pa when the concentration of FPI was increased from 1 wt% to 5 wt%. Similar results have been reported in previous studies on plant-stabilised emulsions, including quinoa and kafirin proteins [28,54]. For example, in quinoa protein stabilised emulsions, the $G'$ increased from ~100 Pa to ~580 Pa when the concentration of QPI increased from 1 wt% to 5 wt%. As shown in Fig. 3, the oil droplets with smaller size and more compact packing at higher concentrations of FPI may result in a greater gel strength [48].

The impact of pH value on the rheological properties of the FPI stabilised emulsions was also measured as shown in Fig. 6**F** which summarized the $G'$ at 1 Hz for different pH values. Emulsions prepared by FPI at pH 7 exhibited the highest $G'$ value (~2800 Pa) followed by at pH 9 (~1500 Pa), pH 3 (~1100 Pa), and pH 5 (~500 Pa). The weakest gel strength at pH 5 could be attributed to the large size and loose packing of oil droplets as revealed by the CLSM observations. Interestingly, although the emulsions prepared by FPI at pH 3, 7 and 9 exhibited a similar droplet size distribution (Figs. 5**B and** 5**E**), their rheological properties varied. It has been previously suggested that in a highly structured emulsion system, oil droplet size distribution is not the only structural parameter influencing rheology of emulsions. Other factors such as interdroplets interactions and protein aggregates in aqueous phase may also play key roles [28,49,66].

As shown in Fig. 6**I**, adding 200 mM NaCl increased the gel strength of 3 wt% FPI (pH 7) stabilised emulsions compared to the sample in the absence of salt. This could be due to enhanced interdroplets interactions due to charge screening effect and/or protein aggregation at the oil-water interface. Similar findings have been reported in karifin stabilised emulsions added with 10–50 mM NaCl [54]. However, an increase

in gel strength was not observed when the emulsion gel was added with 40 mM $CaCl_2$ which could be attributed to large oil droplet sizes and excessive protein aggregation at high ionic strength, which can be observed in the CLSM micrographs (Fig. 3**E**) [32,58].

It is evident that the heat treatment significantly enhanced the gel strength of all FPI-stabilised emulsions (Fig. 6**B, C, and E** ). This was in line with the microstructural characteristics of emulsions as revealed by CLSM (**Figs. 3–4**). The heat treatment induced extensive aggregation of proteins located on surfaces of oil droplets, leading to more compact and denser packing of oil droplets. In addition, and excess proteins in the aqueous phase may also aggregated and act as active fillers in improving the gel strength [3,52]. Similar findings have been reported in previous studies on heat treatment of emulsions stabilised by canola protein isolates [48] and quinoa protein isolates [28].

### 3.7. *Large deformation rheological properties FPI stabilised emulsion gels*

Large deformation rheological behaviour and structural breakdown characteristics of emulsions can be determined by the *strain-sweep* measurements and the results are shown in Fig. 7. For all the samples, at small strain amplitude within the linear viscoelastic region (LVR), $G'$ and $G''$ were found to be independent of strain amplitude. In addition, $G'$ was greater than $G''$ within the LVR, indicating a gel-like network structure with a predominant elastic behaviour [67]. When the strain amplitude was beyond the LVR, the $G'$ values of all samples were dropped remarkably, suggesting the onset of structural disintegration. In some samples such as emulsions stabilised by 1, 3 and 5 wt% FPI before and after the heat treatment, the $G''$ values of samples increased and reached local maximum values then decreased sharply with the strain increase, indicating the type *III* nonlinear behaviour (weak strain overshoot) [68]. The overshoot of $G''$ has been also observed in previous rheological studies of concentrated emulsions stabilised by QPI [28] and CPI [48]. This could be due to energy dissipation induced by the structural rearrangement under large deformations, but the underlying mechanism is still elusive that needs further studies [69]. When the strain amplitude was further increased, $G''$ decreased much faster than $G'$ until crossover occurs at the breaking stress $\sigma_b$ where $G'=G''$. Beyond the $\sigma_b$, $G''$ was greater than $G'$, which signifies a transition from viscoelastic solid-like behaviour to viscoelastic liquid behaviour due to structural breakdown [70].

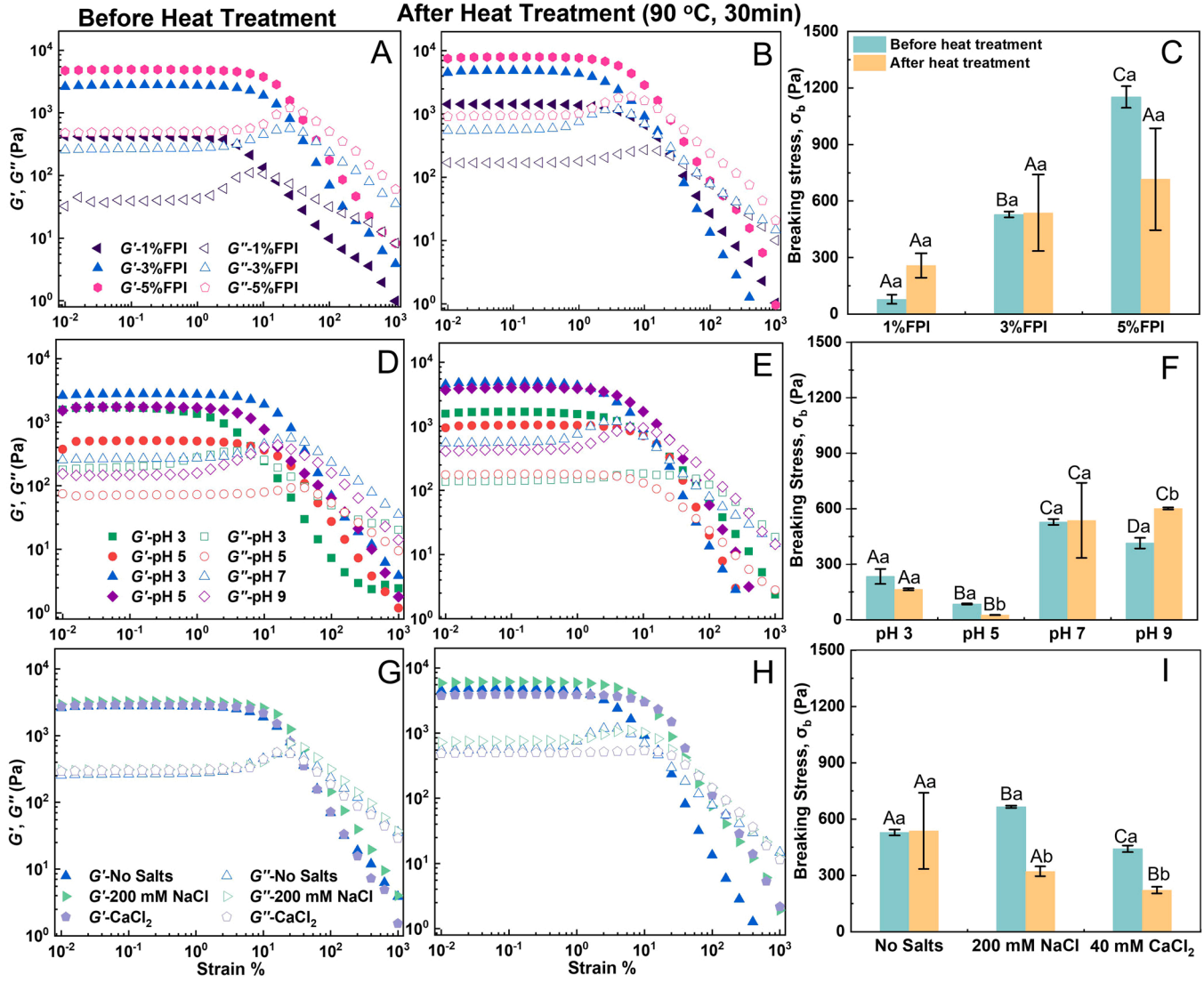


**Fig. 7.** The $G'$ (solid symbols) and $G''$ (empty symbols) as a function of strain amplitude for FPI stabilised emulsions before (A, D, and C) and after (B, E, and F) heat treatment. (C, F, and I) breaking stress of all emulsion gels. Different capital letters above the columns denote significant differences ($P < 0.05$) in emulsions stabilised by FPI at different concentrations, different pHs or adding with salts. The different lowercase letters denote significant differences ($P < 0.05$) between the emulsions before and after the heat treatment.

To better compare the large deformation rheological behaviours of all samples, the breaking stress ($\sigma_b$) of all samples are shown in Fig. 7**C, F and I**. When the FPI concentration increased from 1 wt% to 5 wt%, the $\sigma_b$ showed a substantial increase from ~80–1150 Pa, indicating stronger gels were formed at high FPI concentrations. The effect of pH and salt addition on the $\sigma_b$ also showed a similar trend as $G'$ (1 Hz) as revealed by small deformation rheological studies, indicating the agreement between small and large deformation rheological behaviours.

However, as shown in Fig. 7**C, F and I**, the emulsions after heat treatment did not show similar trends in $\sigma_b$ as compared to $G'$ (1 Hz). Depending on samples, the $\sigma_b$ values were either not significantly changed (e.g., 3 wt% FPI stabilised emulsions at pH 3, 5 and 7) or increased (e.g., 1 wt% FPI stabilised emulsion at pH 7)/decreased (e.g., 3 wt% FPI stabilised emulsion at pH 7 added with 200 mM NaCl) as compared to samples without the heat treatment. As the large deformation rheological properties of concentrated emulsions are complex and affected by various factors such as interdroplets interactions, motions and rearrangement, further studies are needed to explore in more details [71,72].

### 3.8. 3D printing of FPI stabilised emulsion gels

Rheological results indicated that several FPI-stabilised emulsion gels had great mechanical strength, which are critical for 3D printing. To compare the effects of FPI concentration, pH, salt addition, and heat treatment on the printing performance of FPI stabilised emulsions, the emulsion inks were printed into an octagon-shape geometry as shown in Fig. 8. Increasing FPI concentrations greatly improved the printing performance and the object printed from 3 and 5 wt% FPI stabilised emulsions exhibited sharp boundaries, self-supported structures, even surface quality, and high printing precision (e.g., layers can be clearly observed in high resolutions). In contrast, FPI emulsions stabilised by 1 wt% FPI cannot be 3D printed due to their weak gel strength. 3D printing performance of FPI emulsions were also substantially affected by the pH of FPI. As shown in Fig. 8, emulsions stabilised by FPI at pH 3 and pH 5 showed distinct fluidity and structural collapse after 3D printing, while the printed objects from FPI stabilised emulsions at pH 7 and pH 9 showed excellent dimensional stability and precision. Addition of 200 mM NaCl and 40 mM $CaCl_2$ to the FPI stabilised emulsion inks did not significantly affect the 3D printing performance, and well defined and self-supported structures were maintained.

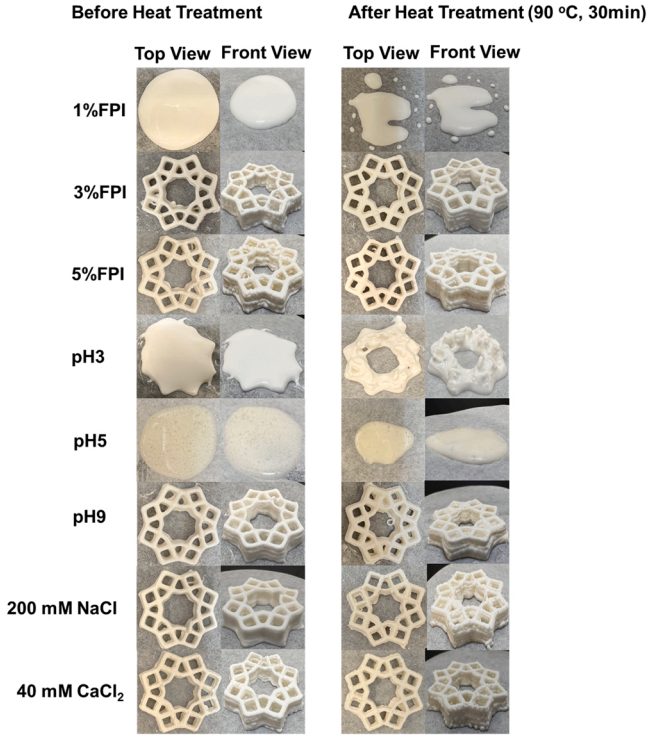


**Fig. 8.** The visual appearance of 5 mm height geometrics shape printed by emulsion gels stabilised by different FPI formulations before and after heat treatment. The images were taken after storage at 20 °C for 1 h.

Heat treatment can improve the 3D printability of some emulsion samples to some extent (e.g. emulsions stabilised by FPI at pH 3), but it still could not form a complete and well-defined structure. Overall, the 3D printing performances of FPI stabilised emulsions were strongly correlated with their rheological properties, which have also been reported in previous 3D extrusion printing studies of emulsion gels stabilised by pea protein-pectin-EGCG complex [73] and whey protein isolates [65]. It is generally believed that high gel strength (e.g., $G' >$ 2000 Pa) and large LVR regimes are critical for supporting previous deposited layers and maintaining the dimensional stabilities. The greater $G'$ values also typically led to better 3D printing performances with enhancement of printing precision and resolution of deposited layers [74,75]. In addition, all the emulsion samples demonstrated a shear thinning behaviour as revealed by the large deformation rheology, which are important for their easy and smooth extrusions from a small diameter printing nozzle [12].

## 4. Conclusions

In conclusion, this study demonstrated that faba bean protein isolate (FPI) was effective in stabilising concentrated O/W emulsions ($\varphi = 0.5$) prepared by high pressure homogenisation. All FPI stabilised emulsions exhibited as viscoelastic gels due to interdroplets aggregation and network formation. The rheological properties and microstructural characteristics of emulsions could be tuned by changing FPI concentration and pH and adding salts (NaCl and $CaCl_2$). As the FPI concentration increased, the storage modulus $G'$ increased. This could be explained by a decrease in oil droplet size, thus tending to form a more closely packed and flocculated emulsion network. It was shown that the FPI demonstrated the worst emulsification capability at pH values close to the isoelectric point (pH 5), as reflected by the high IFT plateau value, large oil droplet size, and weak mechanical strength. The characteristics of emulsions affected by salt addition depended on the salt type. The $G'$ of emulsions slightly increased while the droplet size did not change in the presence of 200 mM NaCl. In contrast, the $G'$ of emulsions remained nearly unchanged, and the droplet size slightly increased after adding 40 mM $CaCl_2$. This could be due to different charge screening effects between monovalent and divalent salts. For all emulsions, the heat treatment (90 °C, 30 min) could substantially improve the mechanical stiffness without markedly affecting the oil droplet size except for the emulsions stabilised by FPI at pH 5. Heat treatment could induce FPI denaturation and aggregation, leading to a thickened interfacial layer and stronger interactions among FPI at the oil-water interface and between non-absorbed FPI in the continuous phase. Finally, the 3D printability of FPI stabilised emulsions was evaluated, which was found to be strongly correlated with their small and large deformation rheological properties. All emulsion samples demonstrated desirable printing performance except the emulsions stabilised by 1 wt% FPI (pH 7) and 3 wt% FPI (pH 5), which showed weak gel strength. Overall, this study demonstrated a potential of using food-grade concentrated emulsion stabilised by FPI as a new material for 3D printing, broadening the applications of plant proteins in the 3D printing. Further work can be performed to explore the applications of 3D printed emulsions for encapsulation and delivery of nutraceuticals and flavours.

## CRediT authorship contribution statement

**Yinxuan Hu:** Methodology, Investigation, Data curation, Formal analysis, Writing – original draft. **Lirong Cheng:** Conceptualization,

Supervision, Investigation, Writing – review & editing. **Sung Je Lee**: Supervision, Writing – review & editing. **Zhi Yang**: Conceptualization, Supervision, Project administration, Writing – review & editing.

## Declaration of Competing Interest

We declare that we have no conflict of interest related to this manuscript.

## Data Availability

Data will be made available on request.

## Acknowledgements

The author Yinxuan Hu thanks the Massey University, New Zealand for a doctoral student scholarship. We would like to acknowledge the technical support of Ms. Lan Luo for helping with SDS-PAGE.

## References

[1] L. Zhao, M. Zhang, B. Chitrakar, B. Adhikari, Recent advances in functional 3D printing of foods: a review of functions of ingredients and internal structures, Crit. Rev. Food Sci. Nutr. 61 (2021) 3489–3503.
[2] F.C. Godoi, B.R. Bhandari, S. Prakash, M. Zhang, Fundamentals of 3D Food Printing and Applications, Academic Press, London, 2019.
[3] X. Li, L. Fan, Y. Liu, J. Li, New insights into food O/W emulsion gels: Strategies of reinforcing mechanical properties and outlook of being applied to food 3D printing, Crit. Rev. Food Sci. Nutr. (2021) 1–23.
[4] J. Suriboot, A.C. Marmo, B.K.D. Ngo, A. Nigam, D. Ortiz-Acosta, B.L. Tai, M. A. Grunlan, Amphiphilic, thixotropic additives for extrusion-based 3D printing of silica-reinforced silicone, Soft Matter 17 (2021) 4133–4142.
[5] M. Shahbazi, H. Jäger, J. Chen, R. Ettelaie, Construction of 3D printed reduced-fat meat analogue by emulsion gels. Part II: Printing performance, thermal, tribological, and dynamic sensory characterization of printed objects, Food Hydrocoll. 121 (2021), 107054.
[6] M. Paciulli, P. Littardi, E. Carini, V.M. Paradiso, M. Castellino, E. Chiavaro, Inulin-based emulsion filled gel as fat replacer in shortbread cookies: Effects during storage, LWT 133 (2020), 109888.
[7] Y. Lu, L. Mao, Z. Hou, S. Miao, Y. Gao, Development of emulsion gels for the delivery of functional food ingredients: From structure to functionality, Food Eng. Rev. 11 (2019) 245–258.
[8] R. Eivazzadeh-Keihan, F. Radinekiyan, A. Maleki, M. Salimi Bani, Z. Hajizadeh, S. Asgharnasl, A novel biocompatible core-shell magnetic nanocomposite based on cross-linked chitosan hydrogels for in vitro hyperthermia of cancer therapy, Int. J. Biol. Macromol. 140 (2019) 407–414.
[9] W. Zhang, R. Taheri-Ledari, F. Ganjali, S.S. Mirmohammadi, F.S. Qazi, M. Saeidirad, A. KashtiAray, S. Zarei-Shokat, Y. Tian, A. Maleki, Effects of morphology and size of nanoscale drug carriers on cellular uptake and internalization process: a review, RSC Adv. 13 (2023) 80–114.
[10] K. Cen, X. Yu, C. Gao, Y. Yang, X. Tang, X. Feng, Effects of quinoa protein Pickering emulsion on the properties, structure and intermolecular interactions of myofibrillar protein gel, Food Chem. 394 (2022), 133456.
[11] K. Cen, C. Huang, X. Yu, C. Gao, Y. Yang, X. Tang, X. Feng, Quinoa protein Pickering emulsion: a promising cryoprotectant to enhance the freeze-thaw stability of fish myofibril gels, Food Chem. 407 (2023), 135139.
[12] X. Li, X. Xu, L. Song, A. Bi, C. Wu, Y. Ma, M. Du, B. Zhu, High internal phase emulsion for food-grade 3D printing materials, ACS Appl. Mater. Interfaces 12 (2020) 45493–45503.
[13] H. Jiang, L. Zheng, Y. Zou, Z. Tong, S. Han, S. Wang, 3D food printing: Main components selection by considering rheological properties, Crit. Rev. Food Sci. Nutr. 59 (2019) 2335–2347.
[14] T.K. Kim, H.I. Yong, S. Jung, Y.B. Kim, Y.S. Choi, Effects of replacing pork fat with grape seed oil and gelatine/alginate for meat emulsions, Meat Sci. 163 (2020), 108079.
[15] R. Zhao, W. Fu, Y. Chen, B. Li, S. Liu, Y. Li, Structural modification of whey protein isolate by cinnamaldehyde and stabilization effect on β-carotene-loaded emulsions and emulsion gels, Food Chem. 366 (2022), 130602.
[16] F. Alavi, L. Chen, Z. Wang, Z. Emam-Djomeh, Consequences of heating under alkaline pH alone or in the presence of maltodextrin on solubility, emulsifying and foaming properties of faba bean protein, Food Hydrocoll. 112 (2021), 106335.
[17] S.Ç. Karataş, D. Günay, S. Sayar, *In vitro* evaluation of whole faba bean and its seed coat as a potential source of functional food components, Food Chem. 230 (2017) 182–188.
[18] J. Boye, F. Zare, A. Pletch, Pulse proteins: processing, characterization, functional properties and applications in food and feed, Food Res. Int. 43 (2010) 414–431.
[19] A.C. Karaca, N. Low, M. Nickerson, Emulsifying properties of chickpea, faba bean, lentil and pea proteins produced by isoelectric precipitation and salt extraction, Food Res. Int. 44 (2011) 2742–2750.
[20] C. Liu, R. Pei, M. Heinonen, Faba bean protein: a promising plant-based emulsifier for improving physical and oxidative stabilities of oil-in-water emulsions, Food Chem. 369 (2022), 130879.
[21] T.G. Burger, Y. Zhang, Recent progress in the utilization of pea protein as an emulsifier for food applications, Trends Food Sci. Technol. 86 (2019) 25–33.
[22] C.E. Gumus, E.A. Decker, D.J. McClements, Impact of legume protein type and location on lipid oxidation in fish oil-in-water emulsions: lentil, pea, and faba bean proteins, Food Res. Int. 100 (2017) 175–185.
[23] M.J. Dille, S.H. Knutsen, K.I. Draget, Gels and gelled emulsions prepared by acid-induced gelation of mixtures of faba bean (*Vicia faba*) protein concentrate and λ-carrageenan, Appl. Food Res. 2 (2022), 100174.
[24] Z.Q. Jiang, J. Wang, F. Stoddard, H. Salovaara, T. Sontag-Strohm, Preparation and characterization of emulsion gels from whole faba bean flour, Foods 9 (2020) 755.
[25] J.Y. Zhang, J.K. Pandya, D.J. McClements, J. Lu, A.J. Kinchla, Advancements in 3D food printing: a comprehensive overview of properties and opportunities, Crit. Rev. Food Sci. Nutr. 62 (2022) 4752–4768.
[26] R.E. Enfield, J.K. Pandya, J. Lu, D.J. McClements, A.J. Kinchla, The future of 3D food printing: Opportunities for space applications, Crit. Rev. Food Sci. Nutr. (2022) 1–14.
[27] M. Langton, S. Ehsanzamir, S. Karkehabadi, X. Feng, M. Johansson, D. P. Johansson, Gelation of faba bean proteins-Effect of extraction method, pH and NaCl, Food Hydrocoll. 103 (2020), 105622.
[28] R. Zhang, L. Cheng, L. Luo, Y. Hemar, Z. Yang, Formation and characterisation of high-internal-phase emulsions stabilised by high-pressure homogenised quinoa protein isolate, Colloids Surf. A: Physicochem. Eng. Asp. 631 (2021), 127688.
[29] M. Felix, A. Romero, C. Carrera-Sanchez, A. Guerrero, Assessment of interfacial viscoelastic properties of Faba bean (*Vicia faba*) protein-adsorbed O/W layers as a function of pH, Food Hydrocoll. 90 (2019) 353–359.
[30] Y. Wang, S. Li, A. Zaheer, Q. Song, Extraction of broad bean protein and effects of NaCl concentration and pH value on its solubility and emulsibility, Trans. Chin. Soc. Agric. Eng. 26 (2010) 380–384.
[31] J.M. Bühler, B.L. Dekkers, M.E. Bruins, A.J. Van Der Goot, Modifying faba bean protein concentrate using dry heat to increase water holding capacity, Foods 9 (2020) 1077.
[32] Z. Yang, L. de Campo, E.P. Gilbert, R. Knott, L. Cheng, B. Storer, X. Lin, L. Luo, S. Patole, Y. Hemar, Effect of NaCl and CaCl2 concentration on the rheological and structural characteristics of thermally-induced quinoa protein gels, Food Hydrocoll. 124 (2022), 107350.
[33] U.K. Laemmli, Cleavage of structural proteins during the assembly of the head of bacteriophage T4, Nature 227 (1970) 680–685.
[34] M. Vogelsang-O'Dwyer, I.L. Petersen, M.S. Joehnke, J.C. Sørensen, J. Bez, A. Detzel, M. Busch, M. Krueger, J.A. O'Mahony, E.K. Arendt, Comparison of Faba bean protein ingredients produced using dry fractionation and isoelectric precipitation: Techno-functional, nutritional and environmental performance, Foods 9 (2020) 322.
[35] L. Luo, L. Cheng, R. Zhang, Z. Yang, Impact of high-pressure homogenization on physico-chemical, structural, and rheological properties of quinoa protein isolates, Food Struct. 32 (2022), 100265.
[36] A.M.M. da Silva, F.S. Almeida, A.C.K. Sato, Functional characterization of commercial plant proteins and their application on stabilization of emulsions, J. Food Eng. 292 (2021), 110277.
[37] N. Péron, R. Mészáros, I. Varga, T. Gilányi, Competitive adsorption of sodium dodecyl sulfate and polyethylene oxide at the air/water interface, J. Colloid Interface Sci. 313 (2007) 389–397.
[38] E. Kaspchak, M.A.S. de Oliveira, F.F. Simas, C.R.C. Franco, J.L.M. Silveira, M. R. Mafra, L. Igarashi-Mafra, Determination of heat-set gelation capacity of a quinoa protein isolate (Chenopodium quinoa) by dynamic oscillatory rheological analysis, Food Chem. 232 (2017) 263–271.
[39] O. Nivala, O.E. Mäkinen, K. Kruus, E. Nordlund, D. Ercili-Cura, Structuring colloidal oat and faba bean protein particles via enzymatic modification, Food Chem. 231 (2017) 87–95.
[40] A. Singhal, A.C. Karaca, R. Tyler, M. Nickerson, Pulse proteins: from processing to structure-function relationships, Grain Legumes 55 (2016).
[41] J. Zhang, Q. Liu, Q. Chen, F. Sun, H. Liu, B. Kong, Synergistic modification of pea protein structure using high-intensity ultrasound and pH-shifting technology to improve solubility and emulsification, Ultrason. Sonochem. 88 (2022), 106099.
[42] I. Otegui, A. Fernández-Quintela, A.D. Diego, C. Cid, M. Macarulla, M. Partearroyo, Properties of spray-dried and freeze-dried faba bean protein concentrates, Int. J. Food Sci. Technol. 32 (1997) 439–443.
[43] N.F. Campbell, F.F. Shih, W.E. Marshall, Enzymic phosphorylation of soy protein isolate for improved functional properties, J. Agric. Food Chem. 40 (1992) 403–406.
[44] L. Amagliani, T.M. van de Langerijt, C. Morgenegg, L. Bovetto, C. Schmitt, Influence of charged and non-charged co-solutes on the heat-induced aggregation of soy and pea proteins at pH 7.0, Food Hydrocoll. (2022), 108392.
[45] C.H. Tang, Globular proteins as soft particles for stabilizing emulsions: Concepts and strategies, Food Hydrocoll. 103 (2020), 105664.
[46] F. Keivaninahr, P. Gadkari, K.Z. Benis, M. Tulbek, S. Ghosh, Prediction of emulsification behaviour of pea and faba bean protein concentrates and isolates from structure–functionality analysis, RSC Adv. 11 (2021) 12117–12135.
[47] C. Chang, S. Tu, S. Ghosh, M. Nickerson, Effect of pH on the inter-relationships between the physicochemical, interfacial and emulsifying properties for pea, soy, lentil and canola protein isolates, Food Res. Int. 77 (2015) 360–367.
[48] Y.R. Tang, S. Ghosh, Stability and rheology of canola protein isolate-stabilized concentrated oil-in-water emulsions, Food Hydrocoll. 113 (2021), 106399.

[49] Y.Q. Zhu, X. Chen, D.J. McClements, L. Zou, W. Liu, Pickering-stabilized emulsion gels fabricated from wheat protein nanoparticles: Effect of pH, NaCl and oil content, J. Dispers. Sci. Technol. 39 (2018) 826–835.
[50] Z. Jiang, M. Pulkkinen, Y. Wang, A.M. Lampi, F.L. Stoddard, H. Salovaara, V. Piironen, T. Sontag-Strohm, Faba bean flavour and technological property improvement by thermal pre-treatments, LWT-Food Sci. Technol. 68 (2016) 295–305.
[51] A. Kimura, T. Fukuda, M. Zhang, S. Motoyama, N. Maruyama, S. Utsumi, Comparison of physicochemical properties of 7S and 11S globulins from pea, fava bean, cowpea, and french bean with those of soybean-french bean 7S globulin exhibits excellent properties, J. Agric. Food Chem. 56 (2008) 10273–10279.
[52] Y. Xu, C. Tang, T. Liu, R. Liu, Ovalbumin as an outstanding Pickering nanostabilizer for high internal phase emulsions, J. Agric. Food Chem. 66 (2018) 8795–8804.
[53] C. Sun, S. Gunasekaran, Effects of protein concentration and oil-phase volume fraction on the stability and rheology of menhaden oil-in-water emulsions stabilized by whey protein isolate with xanthan gum, Food Hydrocoll. 23 (2009) 165–174.
[54] J. Xiao, A.J.P. Gonzalez, Q. Huang, Kafirin nanoparticles-stabilized Pickering emulsions: Microstructure and rheological behavior, Food Hydrocoll. 54 (2016) 30–39.
[55] A. Gharsallaoui, E. Cases, O. Chambin, R. Saurel, Interfacial and emulsifying characteristics of acid-treated pea protein, Food Biophys. 4 (2009) 273–280.
[56] A. Sarkar, H. Kamaruddin, A. Bentley, S. Wang, Emulsion stabilization by tomato seed protein isolate: Influence of pH, ionic strength and thermal treatment, Food Hydrocoll. 57 (2016) 160–168.
[57] X. Zhang, Y. Lei, X. Luo, Y. Wang, Y. Li, B. Li, S. Liu, Impact of pH on the interaction between soybean protein isolate and oxidized bacterial cellulose at oil-water interface: dilatational rheological and emulsifying properties, Food Hydrocoll. 115 (2021), 106609.
[58] X. Zhang, S. Zhang, M. Zhong, B. Qi, Y. Li, Soy and whey protein isolate mixture/calcium chloride thermally induced emulsion gels: Rheological properties and digestive characteristics, Food Chem. 380 (2022), 132212.
[59] D.J. McClements, Protein-stabilized emulsions, Curr. Opin. Colloid Interface Sci. 9 (2004) 305–313.
[60] D. White, I. Fisk, J. Mitchell, B. Wolf, S. Hill, D. Gray, Sunflower-seed oil body emulsions: rheology and stability assessment of a natural emulsion, Food Hydrocoll. 22 (2008) 1224–1232.
[61] Y. Cheng, Y. Fu, L. Ma, P.L. Yap, D. Losic, H. Wang, Y. Zhang, Rheology of edible food inks from 2D/3D/4D printing, and its role in future 5D/6D printing, Food Hydrocoll. (2022), 107855.
[62] S. Banerjee, S. Bhattacharya, Food gels: gelling process and new applications, Crit. Rev. Food Sci. Nutr. 52 (2012) 334–346.
[63] F. Liu, C.H. Tang, Cold, gel-like whey protein emulsions by microfluidisation emulsification: rheological properties and microstructures, Food Chem. 127 (2011) 1641–1647.
[64] R. Kornet, S. Sridharan, P. Venema, L.M. Sagis, C.V. Nikiforidis, A.J. van der Goot, M.B. Meinders, E. van der Linden, Fractionation methods affect the gelling properties of pea proteins in emulsion-filled gels, Food Hydrocoll. 125 (2022), 107427.
[65] Y. Liu, W. Zhang, K. Wang, Y. Bao, J.M. Regenstein, P. Zhou, Fabrication of gel-like emulsions with whey protein isolate using microfluidization: rheological properties and 3D printing performance, Food and Bioprocess, Technology 12 (2019) 1967–1979.
[66] J. Franco, P. Partal, D. Ruiz-M Rquez, B. Conde, C. Gallegos, Influence of pH and protei thermal treatment on the rheology of pea protein-stabilized oil-in-water emulsions, J. Am. Oil Chem. ' Soc. 77 (2000) 975–984.
[67] Y. Zou, X. Yang, E. Scholten, Rheological behavior of emulsion gels stabilized by zein/tannic acid complex particles, Food Hydrocoll. 77 (2018) 363–371.
[68] K. Hyun, S.H. Kim, K.H. Ahn, S.J. Lee, Large amplitude oscillatory shear as a way to classify the complex fluids, J. Non-Newton. Fluid Mech. 107 (2002) 51–65.
[69] T. Mason, J. Bibette, D. Weitz, Elasticity of compressed emulsions, Phys. Rev. Lett. 75 (1995) 2051.
[70] M. Shahbazi, H. Jäger, S.J. Ahmadi, M. Lacroix, Electron beam crosslinking of alginate/nanoclay ink to improve functional properties of 3D printed hydrogel for removing heavy metal ions, Carbohydr. Polym. 240 (2020), 116211.
[71] S.R. Derkach, Rheology of emulsions, Adv. Colloid Interface Sci. 151 (2009) 1–23.
[72] T.F. Tadros, Fundamental principles of emulsion rheology and their applications, Colloids Surf. A: Physicochem. Eng. Asp. 91 (1994) 39–55.
[73] T. Feng, C. Fan, X. Wang, X. Wang, S. Xia, Q. Huang, Food-grade Pickering emulsions and high internal phase Pickering emulsions encapsulating cinnamaldehyde based on pea protein-pectin-EGCG complexes for extrusion 3D printing, Food Hydrocoll. 124 (2022), 107265.
[74] J.Y. Zhang, J.K. Pandya, D.J. McClements, J. Lu, A.J. Kinchla, Advancements in 3D food printing: a comprehensive overview of properties and opportunities, Crit. Rev. Food Sci. Nutr. (2021) 1–18.
[75] Z. Liu, M. Zhang, B. Bhandari, C. Yang, Impact of rheological properties of mashed potatoes on 3D printing, J. Food Eng. 220 (2018) 76–82.